

# Influences of a high excitation frequency (70 MHz) in the glow discharge technique on the process plasma and the properties of hydrogenated amorphous silicon

F. Finger,<sup>a)</sup> U. Kroll, V. Viret, and A. Shah

*Institut de Microtechnique, Université de Neuchâtel, CH-2000 Neuchâtel, Switzerland*

W. Beyer

*Forschungszentrum Jülich, Institut für Schicht- und Ionentechnik, D-5170 Jülich, Germany*

X.-M. Tang and J. Weber

*Institut de Physique, Université de Neuchâtel, CH-2000 Neuchâtel, Switzerland*

A. Howling and Ch. Hollenstein

*Centre de Recherches en Physiques des Plasmas, Ecole Polytechnique Federal Lausanne, CH-1007 Lausanne, Switzerland*

Hydrogenated amorphous silicon has been prepared at a plasma excitation frequency in the very-high-frequency band at 70 MHz with the glow discharge technique at substrate temperatures between 280 and 50 °C. The structural properties have been studied using hydrogen evolution, elastic recoil detection analysis, and infrared spectroscopy. The films were further characterized by dark and photoconductivity and by photothermal deflection spectroscopy. With respect to films prepared at the conventional frequency of 13.56 MHz considerable differences concerning the electronic and structural properties are observed as the substrate temperature is decreased from 280 to 50 °C. Down to a substrate temperature of 150 °C the electronic film properties change only a little and the total hydrogen content  $c_H$  and the degree of microstructure that can be directly correlated to  $c_H$  increase only moderately. Below 150 °C the electronic properties deteriorate in the usual manner but still the total hydrogen content does not exceed 21 at. % even at a substrate temperature of 50 °C. It is argued that the influence of the higher excitation frequency on the plasma and on the growth kinetics plays a key role in this context by allowing a highly effective dissociation of the process gas with the maximum ion energies remaining at low levels. It is concluded that deposition processes at higher excitation frequencies can have important technological implications by allowing a decrease of the deposition temperature without losses in the material quality.

## I. INTRODUCTION

Hydrogenated amorphous silicon ( $\alpha$ -Si:H) is commonly prepared by the silane-based glow discharge (GD) technique. A plasma excitation frequency of 13.56 MHz is generally used, mainly because of the fact that plasma processing equipment for this industrial frequency is readily available. Until recently, little research had been done to study the effect of the excitation frequency on the deposition process and on the electronic properties of the resulting films. It was believed that the excitation frequency would not have a major influence on the growth and the properties of  $\alpha$ -Si:H, mainly because for typical silane plasma conditions at 13.56 MHz, one is above the ion plasma frequency. This means that the ions are practically stationary and so a further increase of the excitation frequency would have no direct influence on the ions in the bulk plasma volume. It cannot, however, be deduced that higher excitation frequencies are unimportant for two reasons: first, the energy-transfer mechanism to the electrons in the bulk plasma has a frequency dependence (e.g., a

resonance at the electron momentum exchange frequency<sup>1</sup>); and second, the frequency strongly affects the plasma/electrode sheath characteristics and, in particular, the sheath potential drop. The potential drop and the ratio of ion transit frequency to excitation frequency determine the ion impact energy distribution on the substrate.<sup>2</sup>

It was therefore an interesting result when our group could demonstrate that the use of higher excitation frequencies in the so-called very-high-frequency (VHF) band (30–300 MHz) leads to favorable conditions for the growth and the properties of  $\alpha$ -Si:H.<sup>3,4</sup> These favorable conditions consist mainly in a considerable increase of the deposition rate of up to 20 Å/s at a frequency of about 70 MHz as compared with typically 2–3 Å/s growth rate with GD at 13.56 MHz. Beyond this frequency the deposition rate was found to drop again to 10 Å/s at 150 MHz. The changes in deposition rate were not accompanied by any deterioration in the electronic properties of the films. Deterioration of the electronic properties is usually observed when one tries to increase the deposition rate with the standard glow discharge at 13.56 MHz. The strong influence of the excitation frequency on the deposition rate has been studied and confirmed in other laboratories.<sup>1,5–8</sup> Moisan *et al.*<sup>1</sup> found a strong influence of the deposition

<sup>a)</sup>Present address: Forschungszentrum Jülich, Institut für Schicht- und Ionentechnik, D-5170 Jülich, Germany.

rate of polymers in plasma depositions excited by surface waves in the range 12–400 MHz. Chatham *et al.*<sup>5,6</sup> studied the excitation frequencies in the range 13.56–110 MHz, using silane and disilane as source gases. For both gases they found a continuous increase of the deposition rate with excitation frequency by a factor of 2.5. Oda and co-workers<sup>7,8</sup> compared GD deposition of *a*-Si:H and  $\mu$ c-Si:H from mixtures of SiH<sub>4</sub> and H<sub>2</sub> at 13.56 and 144 MHz and found a factor of 4 higher deposition rate for *a*-Si:H at the higher excitation frequency. There is therefore convincing evidence that the excitation frequency influences the deposition rate in GD processes. The detailed shape of the deposition rate versus frequency curve can of course be a function of the particular deposition system with its specific features.

No fundamental differences in the optical and electrical properties (e.g., optical absorption, deep defect density, and dark and photoconductivity) of material prepared at high deposition rate with VHF-GD are found as compared with the properties of standard 13.56 MHz material. Meanwhile, *a*-Si:H prepared at high deposition rate with VHF-GD has been successfully implemented into *p-i-n* solar cell structures<sup>4-6</sup> and thin-film field-effect transistors.<sup>9</sup> On the other hand, there are indications from small-angle x-ray scattering (SAXS) experiments that VHF-GD material has a different microstructure in terms of size and distribution of microvoids as compared with 13.56 MHz material.<sup>10</sup>

In addition it was found that the VHF plasma also favors the growth of microcrystalline silicon ( $\mu$ c-Si:H) at considerably lower levels of power and temperature, as compared with the standard glow discharge at 13.56 MHz.<sup>7,11-14</sup> To get further insight into how the change in the plasma excitation frequency might influence the plasma and the film growth kinetics we have studied the correlation between structural and electronic properties of *a*-Si:H films prepared at 70 MHz and compared them with the properties that are generally found in films prepared with the conventional glow discharge at 13.56 MHz. Two series of films have been prepared at fast and slow deposition rates, both series at substrate temperatures  $T_s$  between 280 and 50 °C. The two ranges of deposition rates were chosen to see whether a strong variation of the deposition rate at 70 MHz has similar strong effects on the microstructure as, e.g., the increase of the deposition rate at 13.56 MHz by means of an increase of the discharge power. The film structure and especially the hydrogen bonding and hydrogen content were studied with three different techniques: infrared spectroscopy (IR), hydrogen evolution (EV), and elastic recoil detection analysis (ERDA). The electrical and optical properties were characterized by dark and photoconductivity and by photothermal deflection spectroscopy (PDS).

First results of experiments that concentrated on the incorporation of hydrogen in films prepared at various substrate temperatures at 70 MHz have been published recently.<sup>15</sup> In the present study we shall continue these investigations. More details about the microstructure and the optoelectronic properties will be given here. In addition we

have started a detailed investigation of plasma parameters as a function of the excitation frequency. From these investigations we can propose possible mechanisms that influence the film growth in the VHF-GD process.

## II. EXPERIMENTAL DETAILS

The samples were prepared by the VHF-GD technique at an excitation frequency of 70 MHz from pure SiH<sub>4</sub>. The excitation frequency at 70 MHz was chosen because at this frequency we observe a maximum in the deposition rate.<sup>3</sup> Two series of films were grown at substrate temperatures between 50 and 280 °C keeping the deposition rates at a high ( $R = 10\text{--}20 \text{ \AA/s}$ ) "fast" or low ( $R = 3\text{--}8 \text{ \AA/s}$ ) "slow" level at each deposition temperature. Great care was taken to determine the real surface temperature during deposition. Various calibration runs for standard deposition conditions were performed where the thermal sensor for the electrode heater, which is placed inside the heater close to the electrode surface, was calibrated against a thin thermocouple attached to the substrate surface. Total gas pressure was found to be the most prominent factor determining the gradient between the heater temperature and the "real" surface temperature. Unfortunately it was not possible to measure the surface temperature with the discharge on, due to rf pickup through the thermocouple wires. To obtain an approximation of additional surface heating through rf power dissipation or ion bombardment the surface temperature was measured immediately after cutting off the rf power. The surface temperature was indeed higher by typically about 10 °C immediately after the rf power cutoff and subsequently stabilized at a lower equilibrium value. Therefore, we assume that the quoted temperatures are correct to within 10–20 °C.

Samples were grown on Dow Corning 7059 glass for transport and PDS measurements and on polished (100) Si wafers for the IR, ERDA, and EV measurements. The film thicknesses were typically  $d = 1.5\text{--}4.0 \mu\text{m}$ . Care was taken to measure the film thicknesses with a surface profiler close to the area where the various experiments were performed, as we observe in some cases a considerable inhomogeneity of the film thickness across our standard substrate size of  $83 \times 83 \text{ mm}^2$ . A possible reason for this could be a silane depletion as a consequence of the high deposition rates.

Dark- and photoconductivity measurements were carried out in gap cell configuration using aluminum contacts. For the photoconductivity we used white light of a tungsten halogen lamp and a light intensity of  $60 \text{ mW/cm}^2$ . This was tested to give similar photoconductivities as with a solar light simulator at AM1.5.

For PDS measurements the setup as described recently<sup>16</sup> was modified by using a 250 W halogen lamp in place of the 1000 W xenon lamp. By optimizing the optical lightpath the loss in the intensity could be almost compensated and the signal-to-noise ratio could be improved. PDS of *a*-Si:H yields the optical-absorption spectrum in the sub-band-gap region (0.7–2.0 eV). The characteristic features of the spectrum are an absorption shoulder for photon energies  $h\nu = 0.7\text{--}1.3 \text{ eV}$  and an exponential absorption

band at 1.2 eV,  $\alpha_D$ ; Fig. 2(b) shows the characteristic energy  $E_0$  of the absorption edge measured with PDS. For the PDS experiments only some representative samples preferably thicker than 2  $\mu\text{m}$  have been investigated. Note, however, that two samples prepared at  $T_S = 150^\circ\text{C}$  have thicknesses of only 1.2 and 1.7  $\mu\text{m}$ , respectively. Starting from high-quality material prepared at  $T_S = 280^\circ\text{C}$  with a high ratio of photoconductivity to dark conductivity, with a low defect absorption intensity at 1.2 eV of  $\alpha_D = 1\text{--}2\text{ cm}^{-1}$ , and absorption edges with a characteristic energy  $E_0 = 45\text{ meV}$ , we find that all of these sample parameters change little down to substrate temperatures of  $T_S = 150^\circ\text{C}$ . Below that temperature, there is an abrupt change of these material parameters: The photoconductivity drops down to values between  $10^{-9}$  and  $10^{-10}\text{ S/cm}$ , the defect absorption increase to  $\alpha_D = 60\text{ cm}^{-1}$ , and the characteristic energy of the absorption edge becomes  $E_0 = 60\text{ meV}$  at  $T_S = 50^\circ\text{C}$ . This behavior is found for both ranges of deposition rates investigated and no systematic difference was found between films prepared at high and low deposition rates, respectively. The small change down to  $T_S = 150^\circ\text{C}$  is surprising since with the standard glow discharge at 13.56 MHz an optimum deposition temperature for intrinsic  $\alpha\text{-Si:H}$  is usually reported between 230 and 280  $^\circ\text{C}$ , whereas for deposition temperatures below 200  $^\circ\text{C}$  strong deteriorations of material properties are found.

## B. Structural properties

In this subsection we will address the issue of hydrogen bonds (their density and their type) and whether there are internal voids or clusters (e.g., hydrogen) in the material.

### 1. Infrared spectroscopy

Surprising results are also obtained when looking at the hydrogen bonding and hydrogen content. In Fig. 3 infrared transmission spectra of samples grown with fast deposition rates at 70 MHz and at substrate temperatures between 250 and 50  $^\circ\text{C}$  are shown. For clarity the spectra are shifted with respect to each other on the transmission scale. The striking feature is that with decreasing substrate temperature there are only minor contributions of absorption bands at 2080  $\text{cm}^{-1}$  (Si-H, Si-H<sub>2</sub> on internal surfaces), at 890  $\text{cm}^{-1}$  (Si-H<sub>2</sub>), and at 845  $\text{cm}^{-1}$  [(Si-H<sub>2</sub>)<sub>n</sub>]. Strong absorption bands at these wave numbers are usually observed for films prepared at low deposition temperature; this is indicative for a profound microstructure (internal voids) usually found in such films.<sup>25</sup> In addition, the peak absorption at 640  $\text{cm}^{-1}$  that is used for the determination of the total hydrogen content  $c_H$  increases by a factor of 2 only between the film prepared at 250 and at 50  $^\circ\text{C}$ . Again there is no systematic difference in the behavior of the films prepared at fast or slow deposition rates.

### 2. Total hydrogen content

For the determination of the total hydrogen content from IR transmission spectra we have checked the commonly applied procedure<sup>18-20</sup> by measuring the hydrogen content on one set of samples with two other independent

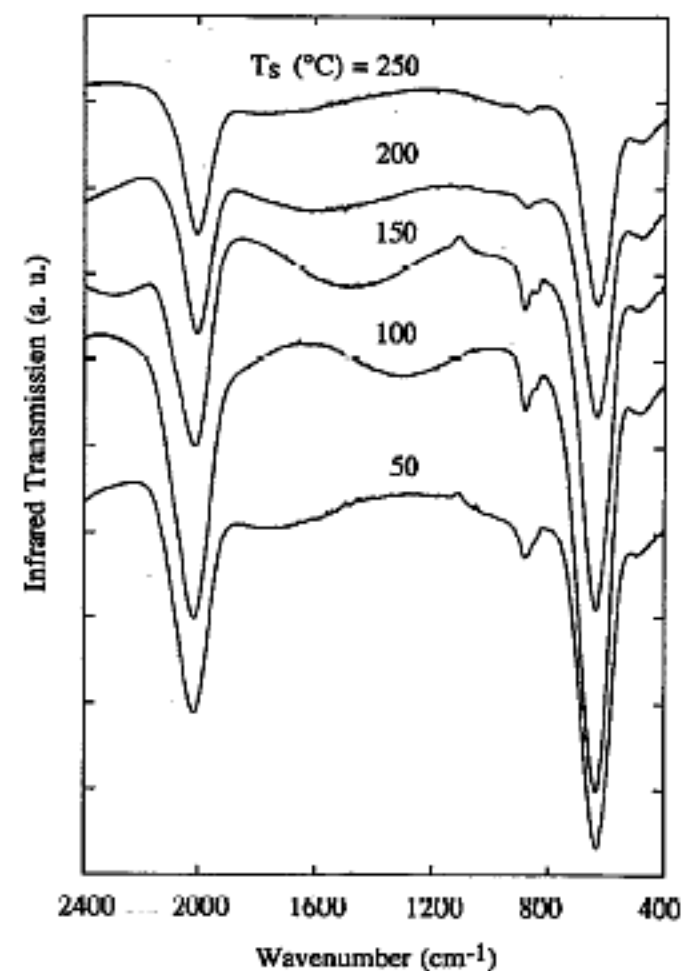


FIG. 3. Infrared transmission spectra for a series of  $\alpha\text{-Si:H}$  films prepared with the VHF-GD technique at fast deposition rates at different substrate temperatures between 50 and 250  $^\circ\text{C}$ . The spectra are shifted with respect to each other.

methods, hydrogen evolution (EV) and elastic recoil detection analysis (ERDA). For this we have chosen the set of samples whose IR spectra are shown in Fig. 3.

The results are shown in Fig. 4. Here, the hydrogen content determined from IR, EV, and ERDA for five samples of the fast deposition series is shown as a function of the substrate temperature. All three methods reveal the

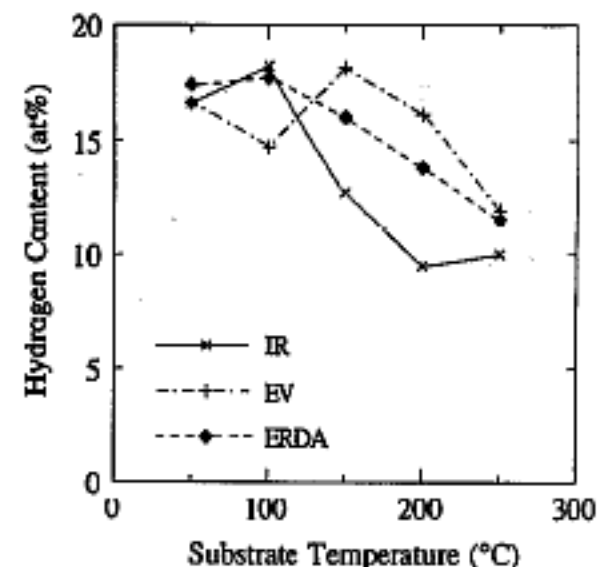


FIG. 4. Total hydrogen content for the  $\alpha\text{-Si:H}$  samples of Fig. 3. The hydrogen content was determined with three different methods: infrared spectroscopy (IR), hydrogen evolution (EV), and elastic recoil detection analysis (ERDA).

band at 1.2 eV,  $\alpha_D$ ; Fig. 2(b) shows the characteristic energy  $E_0$  of the absorption edge measured with PDS. For the PDS experiments only some representative samples preferably thicker than  $2 \mu\text{m}$  have been investigated. Note, however, that two samples prepared at  $T_S = 150^\circ\text{C}$  have thicknesses of only 1.2 and  $1.7 \mu\text{m}$ , respectively. Starting from high-quality material prepared at  $T_S = 280^\circ\text{C}$  with a high ratio of photoconductivity to dark conductivity, with a low defect absorption intensity at 1.2 eV of  $\alpha_D = 1.2 \text{ cm}^{-1}$ , and absorption edges with a characteristic energy  $E_0 = 45 \text{ meV}$ , we find that all of these sample parameters change little down to substrate temperatures of  $T_S = 150^\circ\text{C}$ . Below that temperature, there is an abrupt change of these material parameters: The photoconductivity drops down to values between  $10^{-9}$  and  $10^{-10} \text{ S/cm}$ , the defect absorption increase to  $\alpha_D = 60 \text{ cm}^{-1}$ , and the characteristic energy of the absorption edge becomes  $E_0 = 60 \text{ meV}$  at  $T_S = 50^\circ\text{C}$ . This behavior is found for both ranges of deposition rates investigated and no systematic difference was found between films prepared at high and low deposition rates, respectively. The small change down to  $T_S = 150^\circ\text{C}$  is surprising since with the standard glow discharge at 13.56 MHz an optimum deposition temperature for intrinsic  $\alpha\text{-Si:H}$  is usually reported between 230 and  $280^\circ\text{C}$ , whereas for deposition temperatures below  $200^\circ\text{C}$  strong deteriorations of material properties are found.

## B. Structural properties

In this subsection we will address the issue of hydrogen bonds (their density and their type) and whether there are internal voids or clusters (e.g., hydrogen) in the material.

### 1. Infrared spectroscopy

Surprising results are also obtained when looking at the hydrogen bonding and hydrogen content. In Fig. 3 infrared transmission spectra of samples grown with fast deposition rates at 70 MHz and at substrate temperatures between 250 and  $50^\circ\text{C}$  are shown. For clarity the spectra are shifted with respect to each other on the transmission scale. The striking feature is that with decreasing substrate temperature there are only minor contributions of absorption bands at  $2080 \text{ cm}^{-1}$  (Si-H, Si-H<sub>2</sub> on internal surfaces), at  $890 \text{ cm}^{-1}$  (Si-H<sub>2</sub>), and at  $845 \text{ cm}^{-1}$  [(Si-H<sub>2</sub>)<sub>n</sub>]. Strong absorption bands at these wave numbers are usually observed for films prepared at low deposition temperature; this is indicative for a profound microstructure (internal voids) usually found in such films.<sup>25</sup> In addition, the peak absorption at  $640 \text{ cm}^{-1}$  that is used for the determination of the total hydrogen content  $c_H$  increases by a factor of 2 only between the film prepared at 250 and at  $50^\circ\text{C}$ . Again there is no systematic difference in the behavior of the films prepared at fast or slow deposition rates.

### 2. Total hydrogen content

For the determination of the total hydrogen content from IR transmission spectra we have checked the commonly applied procedure<sup>18-20</sup> by measuring the hydrogen content on one set of samples with two other independent

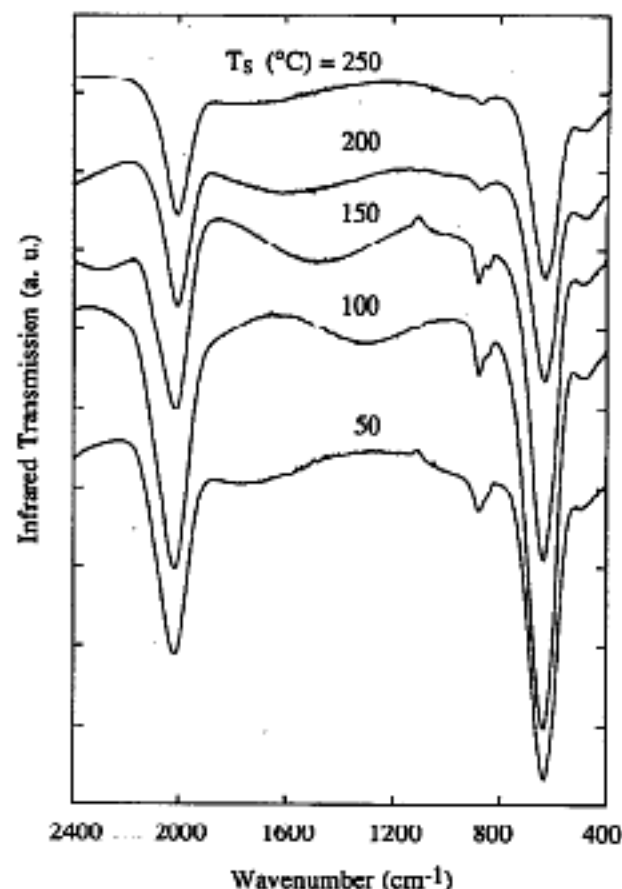


FIG. 3. Infrared transmission spectra for a series of  $\alpha\text{-Si:H}$  films prepared with the VHF-GD technique at fast deposition rates at different substrate temperatures between 50 and  $250^\circ\text{C}$ . The spectra are shifted with respect to each other.

methods, hydrogen evolution (EV) and elastic recoil detection analysis (ERDA). For this we have chosen the set of samples whose IR spectra are shown in Fig. 3.

The results are shown in Fig. 4. Here, the hydrogen content determined from IR, EV, and ERDA for five samples of the fast deposition series is shown as a function of the substrate temperature. All three methods reveal the

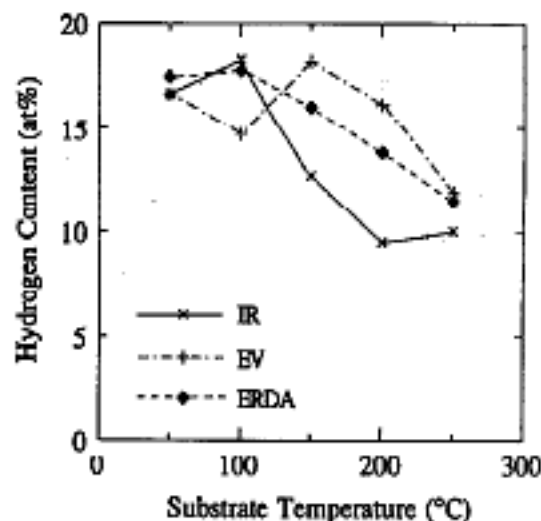


FIG. 4. Total hydrogen content for the  $\alpha\text{-Si:H}$  samples of Fig. 3. The hydrogen content was determined with three different methods: infrared spectroscopy (IR), hydrogen evolution (EV), and elastic recoil detection analysis (ERDA).

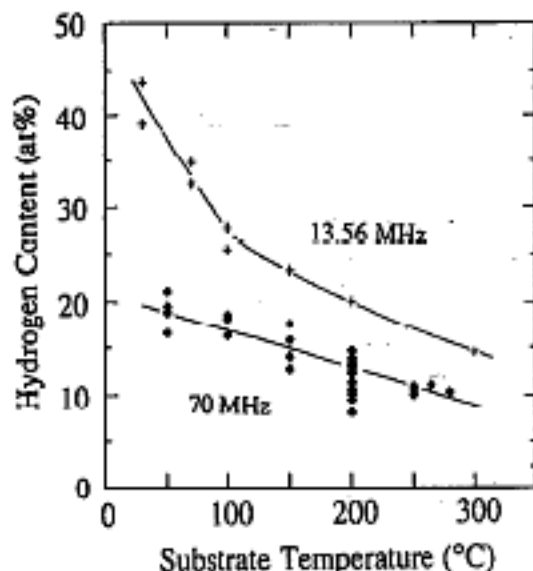


FIG. 5. Total hydrogen content in  $\alpha$ -Si:H films prepared at 70 and at 13.56 MHz (Ref. 25) as a function of the deposition temperature.

same trend: an increase of  $c_H$  from 10 at. % at  $T_S = 250^\circ\text{C}$  to values not exceeding 20 at. % at  $T_S = 50^\circ\text{C}$ . However, when looking for relative accuracy, there is some scatter in the  $c_H$  data determined by the three different methods, each having a typical resolution of  $\pm 15\%$  for the hydrogen content.

Some problems that can occur when comparing the three methods shall be indicated: The general applicability of IR transmission spectra of  $\alpha$ -Si:H for the determination of  $c_H$  has been questioned by several authors—mainly due to the fact that the oscillator strength of the Si—H bonds could be a function of the microstructure of the films and could vary with the hydrogen content itself. EV and ERDA give the hydrogen content in atom density and the atomic percentage has to be calculated by taking into account a variation in the mass density with the hydrogen content. This has been taken care of here using the correlation as given by Beyer.<sup>25</sup> Finally for IR and EV the film thickness and/or the volume of the films must be known accurately. This can lead in the present study to problems especially for the EV measurements on films prepared at low substrate temperatures as it was found that those films have a high internal stress with a tendency to peel off. Accounting for all these uncertainties and considering the absolute accuracy of each method the overall agreement is encouraging. Measurements of the hydrogen content with EV and IR on additional samples confirm this agreement. In summary we find no systematic differences between the different methods used to determine  $c_H$ .

Very similar trends for the hydrogen content  $c_H$  and the infrared spectra as a function of the deposition temperature  $T_S$  are found for the slow deposition series. Data for  $c_H$  for the two series are summarized in Fig. 5. For simplicity, only  $c_H$  data from IR are shown here. Data deduced from the other methods show the same trend (within the experimental error discussed above). For all samples, no matter if prepared at high or at low deposition rates, the hydrogen content does not exceed 21 at. % even at  $T_S = 50^\circ\text{C}$ . For comparison,  $c_H$  data for samples pre-

pared at 13.56 MHz taken from Ref. 25 are also shown in Fig. 5. For samples prepared at  $T_S = 250$ – $300^\circ\text{C}$ , the hydrogen content is typically between 10 and 15 at. % for both plasma excitation frequencies. But there is a clear difference in the hydrogen content at low  $T_S$ . For 13.56 MHz values between 40 and 50 at. % are not unusual whereas in our films  $c_H$  does not exceed 21 at. %.

### 3. Microstructure

Looking at the small increase of  $c_H$  when lowering the deposition temperature it is not surprising that there are only small contributions from infrared absorption bands at 2080, 890, and 845  $\text{cm}^{-1}$ . It has been demonstrated earlier<sup>22</sup> that the indication of microstructure in the IR spectra is strongly correlated to the total hydrogen content itself. The reason for this is that the  $\alpha$ -Si:H network can only absorb H up to a certain concentration in the compact bulk material. As one puts in more H, clustering and the formation of voids sets in. In our case this means that, for the VHF films studied here,  $c_H$  and not primarily  $T_S$  will determine the microstructure (similar to the situation in  $\alpha$ -Si:H films prepared by sputtering at low temperature where  $c_H$  can be controlled by the hydrogen partial pressure during the deposition<sup>22</sup>). Considering the IR absorption mode at 2080  $\text{cm}^{-1}$  as a measure of H cluster or voids, the amount of microstructure can be defined from IR spectra by calculating the ratio  $R$  of the integrated absorption bands at 2080 and 2000  $\text{cm}^{-1}$ .<sup>22,26</sup>

$$R = I_{2080} / (I_{2080} + I_{2000}).$$

The use of this relation for the determination of the amount of microstructure has become very popular recently. However, it should be noted that this ratio does not stand for the ratio of Si—H in internal voids to the total number of Si—H bonds. The reason for this is simply that the oscillator strengths for both types of bonding differ considerably,<sup>27</sup> such that even small contributions of the IR absorption at 2080  $\text{cm}^{-1}$  actually correspond to a large amount of hydrogen in internal voids. This means that the ratio  $R$  as given above underestimates the percentage of microvoids. Here we shall still use the ratio  $R$  as defined above for two reasons: (i) a comparison with data given by other authors is easier, and (ii) the exact values of the oscillator strengths are still a matter of debate and can in addition vary with the microstructure. We have calculated the ratio  $R$  by deconvoluting the IR absorption band in the region 2000–2080  $\text{cm}^{-1}$  into two Gaussian lines and integrating each line. In Fig. 6 the ratio  $R$  is plotted versus the total hydrogen content. Although there is considerable scatter in the data—which might be due to a large extent to uncertainties in the deconvolution of the 2000/2080 absorption mode—we see the expected correlation between the hydrogen content and the amount of microstructure.

### 4. Hydrogen evolution

Hydrogen evolution is another sensitive method for the investigation of microstructure in  $\alpha$ -Si:H. Typical evolution spectra of films prepared at low  $T_S$  at 13.56 MHz show two

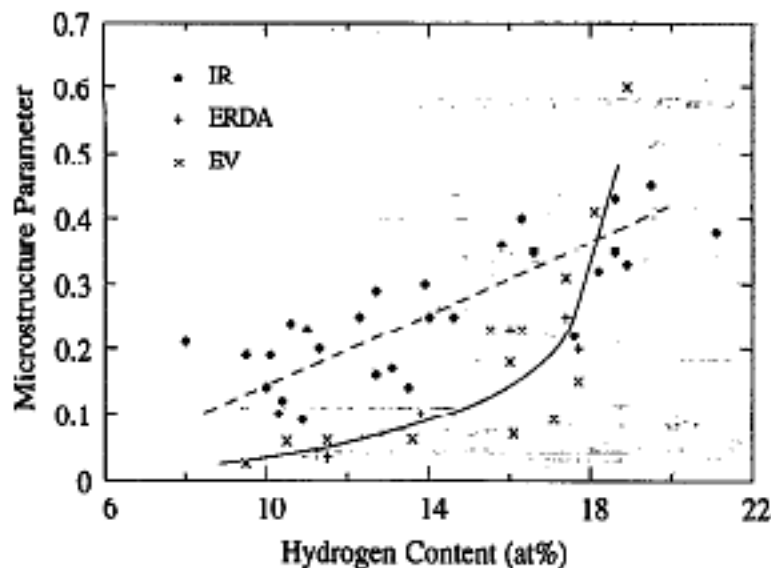


FIG. 6. Microstructure parameter  $R$ ,  $N_{LT}/N_{HT}$ , and  $c_{AM}/c_M$  determined from IR, EV, and ERDA, respectively, as a function of the total hydrogen content in  $\alpha$ -Si:H prepared at various deposition temperatures at 70 MHz.

distinct evolution peaks near  $T = 370^\circ\text{C}$  (LT peak) and  $T = 600^\circ\text{C}$  (HT peak), the latter depending on film thickness. The first peak is attributed to desorption of  $\text{H}_2$  from internal surfaces followed by a rapid exodiffusion of molecular hydrogen through a void network. The second peak is associated with the diffusion of atomic hydrogen in compact material.<sup>22,25</sup> Usually there is a strong correlation between the ratio  $R$  as defined from the deconvolution of the IR spectra and the amount of hydrogen that is evolved in the low-temperature evolution process.<sup>22</sup> A high  $R$  and a high LT peak both indicate a material rich in voids.

In Figs. 7(a) and 7(b) evolution spectra of films prepared by VHF-GD at various substrate temperatures are shown for the two series of films prepared at different deposition rates. A low-temperature effusion peak near  $370^\circ\text{C}$  is identifiable only for  $T_S = 50^\circ\text{C}$  material of the fast series while all other samples of both series reveal a more or less pronounced shoulder at this temperature. From this latter result we conclude that some degree of microstructure is present in all cases. The least microstructure is present for  $T_S = 250^\circ\text{C}$  material. Figure 7(c) shows the temperature  $T_M$  of the maximum effusion rate of the high-temperature peak as a function of the film thickness  $d$ . Except for two films of the slow series, the high-temperature peaks follow closely the film thickness dependence of ( $T_S = 300^\circ\text{C}$ ) 13.56 MHz material<sup>25</sup> governed by diffusion of atomic hydrogen with a diffusion coefficient  $D = 3 \times 10^{-2} \exp(-1.6 \text{ eV}/kT) \text{ cm}^2/\text{s}$ . This result suggests that at the temperature of HT evolution our material is compact on the scale of the film thickness. The presence of both low- and high-temperature hydrogen effusion processes for the same samples is attributed to a film reconstruction process at intermediate temperatures.<sup>22</sup> Incomplete reconstruction resulting in the presence of voids or interfaces that limit the effective hydrogen diffusion length to dimensions less than the film thickness can explain the relatively low  $T_M$  of two samples of the slow series. For both series of films, addi-

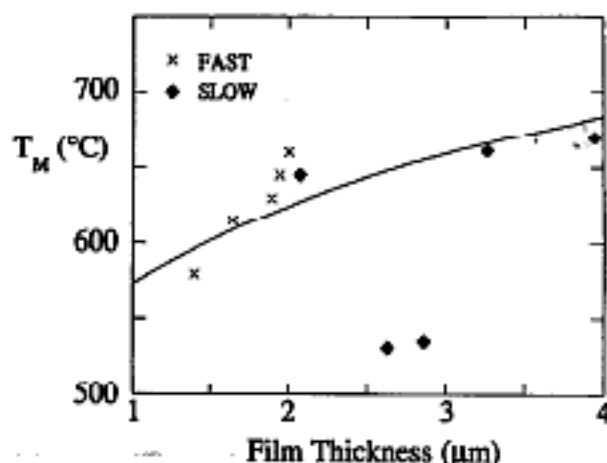
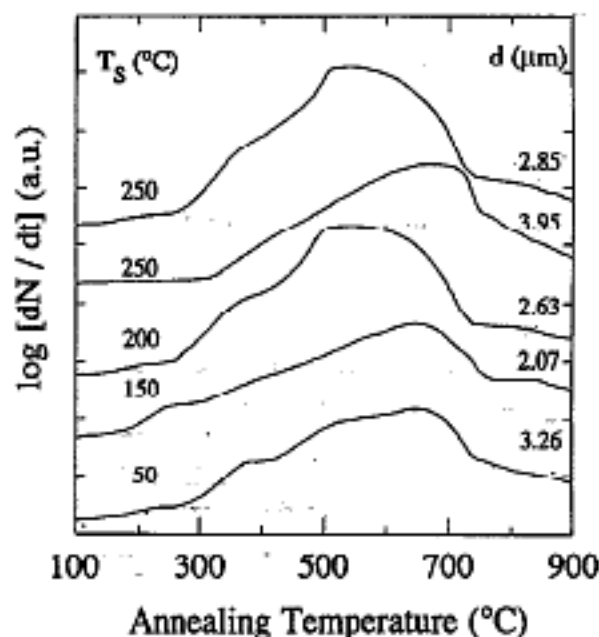
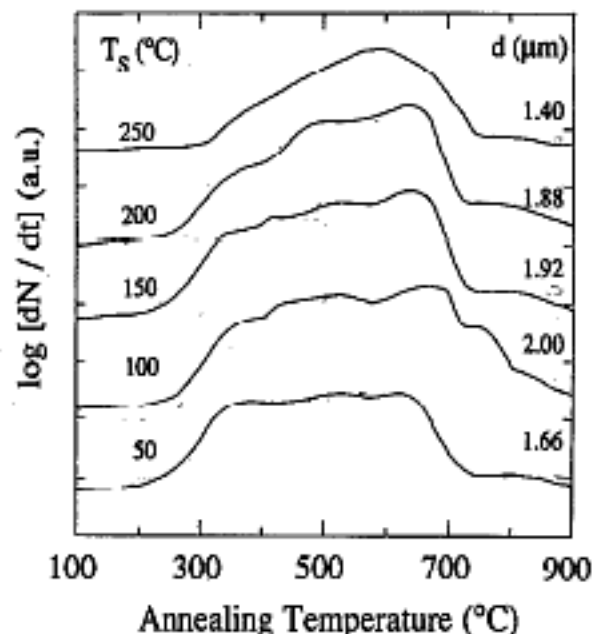


FIG. 7. Hydrogen evolution (EV) spectra of  $\alpha$ -Si:H prepared at 70 MHz with (a) fast or (b) slow deposition rates at substrate temperatures between  $50$  and  $250^\circ\text{C}$ . The heating rate was  $20^\circ\text{C}/\text{min}$ . (c) temperature  $T_M$  of the high-temperature effusion maximum vs the film thickness. The full line is calculated using a hydrogen constant  $D = 3 \times 10^{-2} \exp(-1.6/kT) \text{ cm}^2 \text{ s}^{-1}$ .

tional effusion peaks or shoulders occur in the  $450$ – $550^\circ\text{C}$  range. Although usually not visible in high-quality 13.56 MHz material, similar evolution peaks have been reported for  $\alpha$ -Si:H with a microstructure.<sup>28</sup> Again we attribute

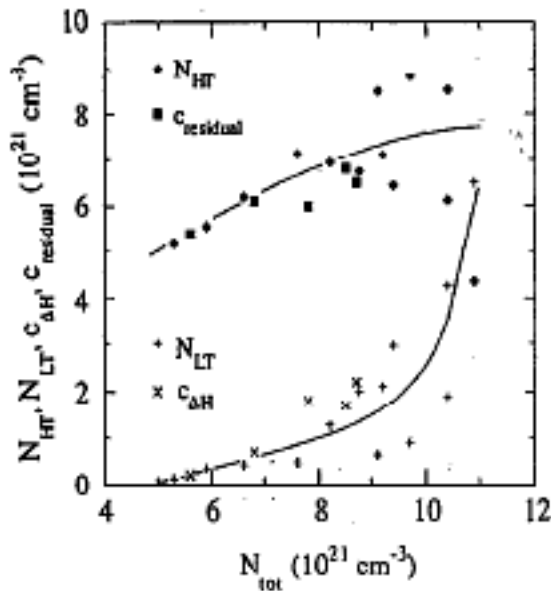


FIG. 8. Hydrogen evolved from  $\alpha$ -Si:H in the low- ( $N_{LT}$ ) and in the high- ( $N_{HT}$ ) temperature evolution process determined from EV; and hydrogen evolved up to 400 °C ( $c_{dH}$ ) and remaining hydrogen after annealing to 400 °C ( $c_{residual}$ ) determined from ERDA vs total hydrogen density  $N_{tot}$ .

these structures to film reconstruction phenomena although other explanations have been given.<sup>28</sup>

In order to obtain a qualitative indication on the amount of hydrogen that is evolved at low and at high temperatures and that could be associated with hydrogen incorporated at void surfaces and in the bulk, respectively, the following procedure is employed: The EV spectra are integrated between the onset of the evolution and  $T = 450$  °C, the approximate temperature of film reconstruction,<sup>25</sup> and between  $T = 450$  °C and the end of the spectra. This leads to the hydrogen densities  $N_{LT}$  and  $N_{HT}$ , respectively.

In Fig. 8,  $N_{LT}$  and  $N_{HT}$  are plotted versus the total hydrogen density  $N_{tot}$ . Despite the fact that the distinction between the LT and HT processes may be somewhat arbitrary, the data agree well with data found for  $\alpha$ -Si:H prepared by other methods.<sup>22</sup> The results indicate a saturation of hydrogen incorporated in compact  $\alpha$ -Si:H at about  $8 \times 10^{21}$  cm<sup>-3</sup> and a sharp onset of the LT evolution due to H<sub>2</sub> diffusing through a void network at about  $N_{tot} = 1 \times 10^{22}$  cm<sup>-3</sup>. In other words, the  $\alpha$ -Si:H network can accommodate only a certain amount of hydrogen in a compact phase. Above a critical concentration  $N_{tot} = 1 \times 10^{22}$  cm<sup>-3</sup> additional hydrogen tends to form clusters and voids. Since the total hydrogen content of our VHF-GD films never exceeds about  $1 \times 10^{22}$  cm<sup>-3</sup> for films prepared at low substrate temperature, the concentration of voids in our low- $T_S$  material is considerably less than for 13.56 MHz films.

Similar to the ratio  $R$  from the IR absorption experiments one can define by the ratio  $N_{LT}/N_{tot}$  a measure of microstructure from the hydrogen evolution studies. The result is also plotted in Fig. 6 as a function of the total hydrogen content. We find that similar to the ratio  $R$  from IR, the ratio  $N_{LT}/N_{tot}$  from hydrogen evolution experiments on our films increases with rising hydrogen content. However, especially at small hydrogen concentrations,

$N_{LT}/N_{tot}$  stays well below the ratio  $R$  and increases strongly only at high hydrogen concentration. The reason for this discrepancy between  $N_{LT}/N_{tot}$  and  $R$  is presumably that the LT evolution appears only for an interconnected void network while infrared absorption measures the presence of all types of voids.

### 5. Elastic recoil detection analysis

In addition, we have investigated the hydrogen exodiffusion with the ERDA experiment. We have measured the hydrogen profile in five samples of the fast series deposited at various deposition temperatures between 250 and 50 °C. First the samples were measured in the as-deposited state; then again after annealing at 400 °C for 30 min. For all samples we find a perfectly flat hydrogen profile before the annealing. After annealing the hydrogen profile drops almost by the same amount  $c_{dH}$  throughout the sample. This is an indication of a remaining void network even in high- $T_S$  films and correlates to the LT evolution spectra that also for high- $T_S$  films show at least a shoulder in the LT region. There is, however, some hydrogen depletion at the film/air interface that is governed by atomic diffusion.

From a stepwise annealing of a sample prepared at  $T_S = 150$  °C up to an annealing temperature of 475 °C,<sup>29</sup> we calculate a hydrogen diffusion coefficient  $D = 4.1 \times 10^{-3} \exp(-1.57 \text{ eV}/kT)$  cm<sup>2</sup>/s; this means that the activation energy for the hydrogen diffusion in compact VHF-GD material is the same as in material prepared at 13.56 MHz at 300 °C (see above).<sup>25</sup> The prefactor  $D_0$  found here is about a factor of 7 smaller than the value found from the hydrogen evolution experiments for 13.56 MHz material prepared at 300 °C, but this difference is certainly not much in view of the different experimental techniques used to calculate the diffusion coefficient. Furthermore it is known that the prefactor  $D_0$  can vary considerably for material with different microstructure.<sup>23,25</sup>

If we correlate the amount of hydrogen  $c_{dH}$  that evolves up to 400 °C with the hydrogen that evolves in the  $N_{LT}$  process in the EV studies, then the ratios  $c_{dH}/c_H$  from ERDA and  $N_{LT}/N_{HT}$  from EV should be about the same. The ratio  $c_{dH}/c_H$  is added to the data in Fig. 6. Again  $c_{dH}/c_H$  increases with the total hydrogen content but, similar to the ratio  $N_{LT}/N_{HT}$  from the EV spectra, the ratio  $c_{dH}/c_H$  from ERDA stays well below the ratio  $R$  from IR.

For another comparison between EV and ERDA we have plotted the amount of hydrogen that evolves upon annealing up to 400 °C ( $c_{dH}$ ) and the amount of hydrogen that remains in the film after annealing ( $c_{residual}$ ) versus the total hydrogen density in Fig. 8. The data from ERDA show the same tendency as the data from EV.

### C. Effective power and electrode voltage

The true power that is dissipated in the plasma is a crucial and by no means easily accessible parameter. Usually, the input power is measured with a directional power meter in the 50  $\Omega$  line just before the matching network. This means that the effective power in the plasma is gen-

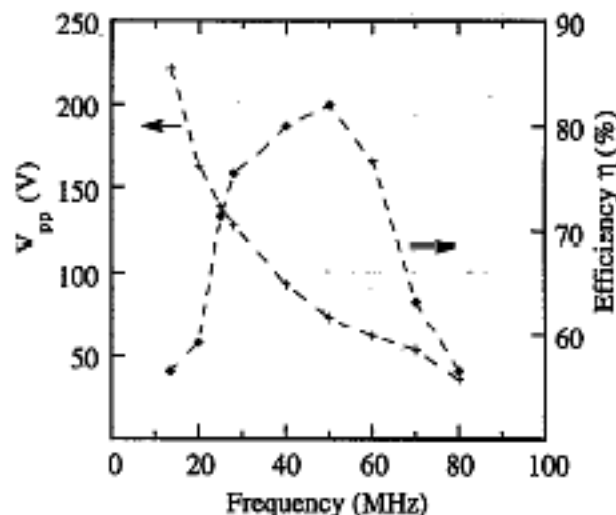


FIG. 9. Efficiency  $\eta$  of power transmission into a silane discharge at constant 15 W input power and peak-to-peak voltage ( $V_{pp}$ ) at the electrodes for constant transmitted power vs the plasma excitation frequency.

erally not known. In particular, since the impedance of the complete system with and without plasma is frequency dependent, the effective plasma power varies with frequency at constant input power. We have estimated the effective power by a subtractive method<sup>30,31</sup> in which the input power without plasma  $P_{vac}$  is subtracted from the total input power  $P_{tot}$  to give the effective power  $P_{eff}$  with the constraint that both  $P_{vac}$  and  $P_{tot}$  are measured for the same electrode voltages. We define a power transfer efficiency  $\eta$  as follows:

$$\eta = [(P_{tot} - P_{vac})/P_{tot}]_{V_{pp} = \text{const}} = P_{eff}/P_{tot}$$

where  $P_{eff}$  is the effective power dissipated in the plasma for a given input power  $P_{tot}$ . This is plotted in Fig. 9 along with the electrode peak-to-peak voltage  $V_{pp}$  for a frequency scan at constant input power 15 W. It is found that the power transfer efficiency in our reactor varies between 55% and 80% over the range of frequencies (10–80 MHz) investigated. The electrode peak-to-peak voltage increases continuously from 50 V at 80 MHz to more than 200 V at 10 MHz.

Following the approach by Köhler, Horne, and Coburn,<sup>32</sup> neglecting collision and ionization in the sheath, one can use the peak-to-peak voltage to estimate the maximum ion energy as  $V_{pp}/4$ . Since  $V_{pp}$  is much higher at low frequency, the maximum ion energies are much higher as well.

## IV. DISCUSSION

### A. High deposition rate and maintenance of material quality

The detailed mechanisms that influence the growth conditions and the resulting structure of *a*-Si:H films via a change in the plasma excitation frequency are not yet well understood.

The most obvious effect that has been found independently by several workers<sup>1,3–8,24</sup> is the strong increase in the deposition rate with frequency. In our case the variation in

the power transfer efficiency with frequency that is presented here can only partly explain the changes in the deposition rate. The decrease in deposition rate beyond 80 MHz in our deposition system can, in fact, be attributed to high-frequency losses. However, in order to explain the initial increase of the deposition rate found in our case<sup>3,24</sup> and for the continuous increase from 13.56 to 110 MHz,<sup>5,6</sup> one has to assume additional frequency-dependent effects on the plasma process. Such effects have been concluded from the theoretical works of Ferreira and Loureiro<sup>33</sup> and Wertheimer and Moisan<sup>34</sup> that propose an increasing high-energy tail in the electron energy distribution function (EEDF) with increasing ratio  $\omega/\nu$  of plasma excitation frequency  $\omega$  to energy collision frequency  $\nu$ . First results for differences in the EEDF in a silane plasma at 13.56 and 144 MHz have been deduced from Langmuir probe and optical emission spectroscopy experiments.<sup>8</sup> A recent study on silane plasmas in the range 13–70 MHz, where special care was taken to control the effective power as the frequency was varied, confirms these findings.<sup>24</sup> However, conclusive experimental evidence for variations in the EEDF with plasma excitation frequency is still lacking and this problem should be topic of further investigation.

For the maintenance of the material quality of *a*-Si:H prepared at high deposition rates with VHF GD an important quantity that must be considered here is the maximum energy of ions impinging on the substrate. High ion energies will lead to sputtering effects and will create defects during the growth. However, one can well imagine that a certain ion bombardment with low-energy ions could be beneficial for the growth by increasing the surface mobility of the radicals and by etching away unfavorably placed species.

As we have seen, the maximum ion energy estimated from the peak-to-peak voltage increases strongly with decreasing frequency, even for constant effective power, i.e., at low frequency there is a much higher ion impact energy on the substrate, which could lead to poor material quality. On the other hand, as mentioned above, a sufficient amount of low-energy ion bombardment is considered to be beneficial for the growth, as it may, e.g., increase the surface mobility and the desorption of reactive species—this mechanism would then be favored at 70 MHz plasmas as compared to 13.56 MHz. Attempting to increase the growth rate at 13.56 MHz by raising the rf input power would simply increase the ion impact energy. At 70 MHz, however, the effective power and, consequently, the growth rate could be increased while keeping the ion impact energy within reasonable limits concomitant with deposition of good quality material.

### B. Effects on the properties of *a*-Si:H

Next let us look at the total hydrogen content in films prepared at low substrate temperatures with the VHF-GD technique. The hydrogen content does not exceed 21 at. % even at 50 °C substrate temperature. For the standard 13.56 MHz deposition, the strong increase of  $c_H$  with decreasing  $T_s$  is explained in the following way. With decreasing substrate temperature we have a decrease in two

quantities: the mobility of reactive species at the surface of the growing film and the hydrogen desorption from the surface.

There is, therefore, a tendency at low substrate temperatures for hydrogen to stick at unfavorable sites and to form H clusters and voids. In this picture, a mechanism that makes hydrogen more mobile could explain the relatively small value of hydrogen built in at low  $T_S$  in the VHF-GD process. From the increase in the deposition rate we conclude that at higher excitation frequencies the dissociation of the process gas for a given input power is much more effective than at 13.56 MHz. This can be achieved with the electrode potentials  $V_{pp}$  remaining at a very low level. Both a high radical density and a low-energy ion flux are beneficial for growth by increasing the desorption rate of hydrogen and by increasing the mobility of species at the growing surface, both without creating defects because of the low ion energy (i.e., the low ion energy is better adapted to the chemical surface activation energies—around 3 eV).

In this context the effect of an increasing excitation frequency is similar to the effect of increasing substrate temperature. Concerning the building in of hydrogen and, correlated with this, the microstructure and the electronic properties, the use of higher excitation frequencies would then permit good quality operation at lower substrate temperatures. Our results on the electronic properties of the films prepared at 70 MHz at substrate temperatures between 150 and 200 °C confirm this, where it should be noted that the deposition conditions have not been optimized for the low deposition temperatures. We find that the electronic properties do not become much worse down to  $T_S = 150$  °C.

Thus, for films prepared at a given substrate temperature below 200 °C at 13.56 MHz and those prepared at 70 MHz we observe clear differences in the properties of *a*-Si:H. Nevertheless, we find for films prepared at 70 MHz that the amount of hydrogen built into the films plays a similar key role in determining the microstructure and thus the electronic properties of *a*-Si:H as in films prepared at 13.56 MHz.<sup>25</sup> Changes in the deposition rate at 70 MHz have no significant influence on the structure and the electronic properties of the *a*-Si:H films. This shows that the deposition rate for *a*-Si:H can be varied over a wide range without changes in the material quality, provided other deposition parameters such as, e.g., the sheath potential can be adjusted.

Finally, we discuss the indications for structural differences between films prepared at 13.56 MHz and those prepared at 70 MHz. As shown in Fig. 6, we have differences in the dependence of the microstructure parameters  $R$ ,  $N_{LT}/N_{tot}$  and  $c_{\Delta H}/c_H$  on the total hydrogen content. Both,  $N_{LT}/N_{tot}$  and  $c_{\Delta H}/c_H$  always stay below  $R$ . This is surprising, since we have mentioned above that the oscillator strength of the Si—H bonds that give rise to the IR absorption at 2080  $\text{cm}^{-1}$  is such that the real amount of hydrogen in the corresponding configuration is underestimated. From the data shown in Fig. 6 one would then have to conclude that only a small amount of the hydrogen from

the 2080  $\text{cm}^{-1}$  mode evolves in the low-temperature evolution process. In the picture of voids, this means that in addition to the interconnected void network that allows the rapid hydrogen exodiffusion at low temperature, we have a large number of medium-sized voids that are not interconnected. Recently, a comparative study of VHF- and rf-GD material with SAXS (Ref. 10) pointed the same way: VHF material has a higher volume fraction of voids and these voids have a wider distribution in void sizes as compared with rf-GD material.

For the uncommon features found in the EV spectra of VHF material an explanation could be that the material investigated here undergoes a stepwise reconstruction during the annealing process. This means that, when starting at low annealing temperature, hydrogen will first desorb from void surfaces and percolate through a void network. At a critical temperature the material partly reconstructs and starts forming larger grains of compact material, blocking void percolation paths. Thus, on the one hand, the rate of the hydrogen evolution via the void percolation decreases as percolation paths are interrupted, on the other hand, the rate of hydrogen evolution via diffusion in the bulk material increases and finally dominates.

## V. SUMMARY AND CONCLUSIONS

In films prepared with VHF-GD at low and high deposition rates and temperatures between 50 and 280 °C we find little deterioration of the optoelectronic properties down to deposition temperatures as low as 150 °C. At the same time, the hydrogen content increases only moderately with decreasing deposition temperature and remains well below the hydrogen content found in samples prepared at low deposition temperatures at 13.56 MHz. Nevertheless we find that the correlation between microstructure and the total hydrogen content in VHF-GD material is similar to the one observed in films prepared by rf-GD. The deposition rate itself, in the series reported on here, is not observed to be correlated to the film structure and the material quality.

Changes in the process plasma as a function of the plasma excitation frequency are considered to be responsible for the favorable growth conditions for *a*-Si:H with VHF-GD. The highly effective process gas decomposition leads to high deposition rates while the maximum ion energies still can be kept at levels close to the chemical energies of the material at the growing surface. This possibility offers additional scope for varying process parameters in a way useful for material preparation.

## ACKNOWLEDGMENTS

We would like to thank S. Dubail, X. Gunashekar, K. Prasad, R. Tschärner, and M. Vanecek for helpful discussions and technical assistance. The work was supported by Swiss Federal Research Grants No. EF-REN (87)9 and No. EF-REN (89)17, and the Swiss National Science Foundation.

- <sup>1</sup>M. Moisan, C. Barbeau, R. Claude, C. M. Ferreira, J. Margot-Chaker, J. Parasczak, A. B. Sa, G. Sauve, and M. R. Wertheimer, *J. Vac. Sci. Technol. B* **9**, 8 (1991).
- <sup>2</sup>D. L. Flamm, *J. Vac. Sci. Technol. A* **4**, 729 (1986).
- <sup>3</sup>H. Curtins, N. Wyrach, and A. Shah, *Electron. Lett.* **23**, 228 (1987).
- <sup>4</sup>D. Fischer, H. Keppner, F. Finger, K. Prasad, A. V. Shah, in *Proceedings of the 10th EC Photovoltaic Solar Energy Conference*, edited by A. Lugue, G. Sala, W. Palz, G. Doe Santos, and P. Helm, Lisbon, 1991, p. 201.
- <sup>5</sup>H. Chatham and P. Bhat, *Mater. Res. Soc. Symp. Proc.* **149**, 447 (1989).
- <sup>6</sup>H. Chatham, P. Bhat, A. Benson, and C. Matovich, *J. Non-Cryst. Solids* **115**, 201 (1989).
- <sup>7</sup>S. Oda, J. Noda, and M. Matsumura, *Mater. Res. Soc. Symp. Proc.* **118**, 117 (1988).
- <sup>8</sup>S. Oda, J. Noda, and M. Matsumura, *Jpn. J. Appl. Phys.* **29**, 1889 (1990).
- <sup>9</sup>S. Oda and M. Yasukawa, *J. Non-Cryst. Solids* **137&138**, 677 (1991).
- <sup>10</sup>A. H. Mahan, Y. Chen, D. L. Williamson, and G. D. Mooney, *J. Non-Cryst. Solids* **137&138**, 65 (1991).
- <sup>11</sup>K. Prasad, F. Finger, H. Curtins, A. Shah, and J. Baumann, *Mater. Res. Soc. Symp. Proc.* **164**, 27 (1989).
- <sup>12</sup>K. Prasad, U. Kroll, F. Finger, A. Shah, and J. Baumann, *Mater. Res. Soc. Symp. Proc.* **219**, 383 (1991).
- <sup>13</sup>F. Finger, K. Prasad, A. Shah, X.-M. Tang, J. Weber, and W. Beyer, *Mater. Res. Soc. Symp. Proc.* **219**, 469 (1991).
- <sup>14</sup>K. Prasad, F. Finger, S. Dubail, A. Shah, and M. Schubert, *J. Non-Cryst. Solids* **137&138**, 681 (1991).
- <sup>15</sup>F. Finger, V. Viret, A. Shah, X.-M. Tang, J. Weber, and W. Beyer, *Mater. Res. Soc. Symp. Proc.* **192**, 583 (1990).
- <sup>16</sup>H. Curtins and M. Favre, in *Amorphous Silicon And Related Materials*, edited by H. Fritzsche (World Scientific, Singapore, 1989), p. 329.
- <sup>17</sup>N. Wyrach, F. Finger, T. J. McMahon, and M. Vanecek, *J. Non-Cryst. Solids* **137&138**, 347 (1991).
- <sup>18</sup>M. H. Brodsky, M. Cardona, and J. J. Cuomo, *Phys. Rev. B* **16**, 3556 (1977).
- <sup>19</sup>A. A. Langford, M. L. Flead, and M. H. Mahan, *Sol. Cells* **27**, 373 (1989).
- <sup>20</sup>H. Shanks, C. J. Fang, L. Ley, M. Cardona, F. J. Demond, and S. Kalbitzer, *Phys. Status Solidi B* **110**, 43 (1980).
- <sup>21</sup>N. Maley and I. Szafranek, *Mater. Res. Soc. Symp. Proc.* **192**, 663 (1989).
- <sup>22</sup>W. Beyer and H. Wagner, *J. Non-Cryst. Solids* **59&60**, 161 (1983).
- <sup>23</sup>X.-M. Tang, J. Weber, Y. Baer, and F. Finger, *Solid State Commun.* **74**, 171 (1990).
- <sup>24</sup>A. A. Howling, J.-L. Dorier, Ch. Hollenstein, U. Kroll, and F. Finger, *J. Vac. Sci. Technol.* (to be published).
- <sup>25</sup>W. Beyer, in *Tetraedrally-Bonded Amorphous Semiconductors*, edited by D. Adler and H. Fritzsche (Plenum, New York, 1985), p. 129.
- <sup>26</sup>A. H. Mahan, P. Raboisson, and R. Tsu, *Appl. Phys. Lett.* **50**, 335 (1987).
- <sup>27</sup>M. Cardona, *Phys. Status Solidi B* **118**, 463 (1983).
- <sup>28</sup>D. K. Biegelsen, R. A. Street, C. C. Tsai, and J. C. Knights, *Phys. Rev. B* **20**, 4839 (1979).
- <sup>29</sup>X.-M. Tang, J. Weber, Y. Baer, and F. Finger, *Phys. Rev. B* **42**, 7277 (1990).
- <sup>30</sup>C. M. Horwitz, *J. Vac. Sci. Technol. A* **1**, 1795 (1983).
- <sup>31</sup>V. A. Godyak and R. B. Piejak, *J. Vac. Sci. Technol. A* **8**, 3833 (1990).
- <sup>32</sup>K. Köhler, D. E. Horne, and J. W. Coburn, *J. Appl. Phys.* **88**, 3350 (1985).
- <sup>33</sup>C. M. Ferreira and J. Loureiro, *J. Phys. D* **17**, 1175 (1984).
- <sup>34</sup>M. R. Wertheimer and M. Moisan, *J. Vac. Sci. Technol. A* **3**, 3634 (1985).